LIMNOLOGY and OCEANOGRAPHY

ASLO

Limnol. Oceanogr. 9999, 2024, 1–15

doi: 10.1002/lno.12761

Organic alkalinity distributions, characteristics, and application to carbonate system calculations in estuarine and coastal systems

Christopher W. Hunt [1*] **Joseph E. Salisbury** [1] **Xuewu Liu** [2] **Robert H. Byrne** [2]

[1]Ocean Process Analysis Laboratory, University of New Hampshire, Durham, New Hampshire, USA
[2]College of Marine Science, University of South Florida, St. Petersburg, Florida, USA

Abstract

The capacity of aquatic systems to buffer acidification depends on the sum contributions of various chemical species to total alkalinity (TA). Major TA contributors are inorganic, with carbonate and bicarbonate considered the most important. However, growing evidence shows that many rivers, estuaries, and coastal waters contain dissolved organic molecules with charge sites that create organic alkalinity (OrgAlk). This study describes the first comparison of (1) OrgAlk distributions and (2) acid–base properties in contrasting estuary-plume systems: the Pleasant (Maine, USA) and the St. John (New Brunswick, CA). The substantial concentrations of OrgAlk in each estuary were sometimes not conservative with salinity and typically associated with very low pH. Two approaches to OrgAlk measurement showed consistent differences, indicating acid–base characteristics inconsistent with the TA definition. The OrgAlk fraction of TA ranged from 78% at low salinity to less than 0.4% in the coastal ocean endmember. Modeling of titration data identified three groups of organic charge sites, with mean acid–base dissociation constants (pK_a) of 4.2 (± 0.5), 5.9 (± 0.7) and 8.5 (± 0.2). These represented 21% (± 9%), 8% (± 5%), and 71% (± 11%) of titrated organic charge groups. Including OrgAlk, pK_a, and titrated organic charge groups in carbonate system calculations improved estimates of pH. However, low and medium salinity, organic-rich samples demonstrated persistent offsets in calculated pH, even using dissolved inorganic carbon and CO_2 partial pressure as inputs. These offsets show the ongoing challenge of carbonate system intercomparisons in organic rich systems whereby new techniques and further investigations are needed to fully account for OrgAlk in TA titrations.

Estuaries are the nexus between terrestrial and oceanic aquatic systems, and the sites of some of the heaviest population densities in the world (Nixon 1995). Estuaries also provide important ecosystem services such as nursery and fishery habitats, filtering and detoxification, and flooding and storm event mitigation (Barbier et al. 2011). However, estuaries are threatened by changing atmospheric conditions (nitrogen deposition, carbon dioxide enrichment), oceanic environmental change (ocean acidification, sea level rise, warming, frequency and intensity of storms), and changes in terrestrially derived inputs (eutrophication, organic matter fluxes, increased runoff).

The cumulative impacts of these changes on estuaries are unclear. On one hand, estuaries are commonly heterotrophic, high CO_2 environments that are more susceptible to acidification than adjacent ocean waters (Cai et al. 2011). The primary sources of acid buffering in ocean water have long been known to be inorganic (e.g., modulated by dissolved carbonate [CO_3^{2-}] and bicarbonate [HCO_3^-] ions; Park 1960), but the contributions of these ions to buffering in estuaries are commonly lower (Hu and Cai 2013). The carbonate/bicarbonate buffer regulates pH and the partial pressure of carbon dioxide (pCO_2) by H^+ exchange equilibria:

$$CO_2 + H_2O \leftrightarrow H_2CO_3 \leftrightarrow H^+ + HCO_3^- \leftrightarrow 2H^+ + CO_3^{2-} \quad (1)$$

While CO_3^{2-} and HCO_3^- ions are the primary contributors to total alkalinity (TA) and pH buffering, other charged species can make significant contributions as well. Organic alkalinity (OrgAlk) has been identified as an important contributor to TA in riverine and low-salinity coastal environments (Hudson-

*Correspondence: chunt@unh.edu

Additional Supporting Information may be found in the online version of this article.

Author Contribution Statement: CWH: Conceptualization; Funding acquisition; Investigation; Project administration; Writing—original draft; Writing—review and editing. JES: Conceptualization; Funding acquisition; Investigation; Writing—review and editing; Supervision. XL: Investigation; Resources; Methodology. RHB: Conceptualization; Funding acquisition; Resources; Supervision; Writing—review and editing; Supervision; Project administration.

Heck & Byrne 2022; Waldbusser and Salisbury 2014) including Gulf of Maine rivers (Hunt et al. 2011), the Kennebec estuary (ME, USA, Hunt et al. 2013), intertidal salt marshes (Song et al. 2020), some southeastern US estuaries (Cai et al. 1998), Baltic Sea estuary waters (Kuliński et al. 2014), Gulf of Mexico estuaries and coastal waters (Yang et al. 2015), and Korean coastal waters (Ko et al. 2016). The term organic alkalinity refers to the contributions of weak organic acids to TA—a contribution that can be modeled in terms of the total concentrations of conjugate organic acids/bases, relevant acid dissociation constants (pK_a), and in situ pH. The contributions of a particular organic acid to TA may be quite different in acidic and alkaline estuaries because the contributions of organic bases to OrgAlk are pH dependent. While organics constitute potentially important alkalinity components, the overall sources and roles of organic acids in driving physiochemical reactions within estuaries remain unclear. Without a better understanding of the interplay between organic and inorganic alkalinity in estuaries and their coastal plumes, the potential of estuaries to respond to acidification threats from both land and sea cannot be determined.

Examinations of aquatic carbonate systems can utilize measurements of TA, pH, dissolved inorganic carbon (DIC), and the partial pressure of carbon dioxide (pCO_2). Measurements of two of these parameters, together with appropriate pK_a values are commonly used to model pH buffering behavior in lakes (Cole et al. 1994; McDonald et al. 2013), rivers (Butman and Raymond 2011; Raymond et al. 2013), estuaries (Borges 2005), and ocean waters (Park 1960). Software packages such as CO2SYS (Lewis and Wallace 1998) and SeaCARB (Gattuso et al. 2021) are available across a wide range of computing platforms to facilitate these calculations. However, if TA is used as one of the inputs for these calculations, and OrgAlk is present in significant quantities, then derived results will be inaccurate (systematically biased). For example, if TA and pH are used to derive pCO_2 and DIC, and OrgAlk is significant, DIC and pCO_2 may both be substantially overestimated (Abril et al. 2014). Recent estimates of CO_2 release from US lakes (McDonald et al. 2013), US rivers (Butman and Raymond 2011), and global rivers (Raymond et al. 2013) modeled CO_2 fluxes from the combination of TA and pH; consequently, our understanding of global terrestrial and estuary CO_2 fluxes is subject to large potential uncertainties due to the effects of OrgAlk.

Estimating the contribution of a charge group to TA requires knowledge of both the concentration of that group and its dissociation constant. The pK_a values of carbonate and bicarbonate are characterized and predictable from salinity, temperature and pressure. The pK_a values of OrgAlk, although influenced by salinity, temperature, and pressure, are not well understood. Studies that have characterized the pK_a of estuary OrgAlk have yielded a continuum of values from less than 4.5 to greater than 7.5, indicating that OrgAlk acid–base chemistry is complex (e.g., Cai et al. 1998; Kuliński et al. 2014; Yang et al. 2015; Ko et al. 2016; Song et al. 2020; Kerr et al. 2023a,b; Song et al. 2023).

In studies of seawater (Dickson 1981) and freshwater (Stumm and Morgan 1995; Drever 1997), TA is discussed as the sum of anions in solution which can be neutralized by strong acid. In both aquatic environments, the pH "equivalence point" has been operationally set at pH 4.5. The definition from Dickson (1981) is presented in Eq. 2, where any species with a pK_a greater than or equal to 4.5 at zero ionic strength is defined as a base (or proton acceptor) while any species with a pK_a less than 4.5 is defined as an acid (or proton donor). This definition has served the oceanographic community well, as the inorganic components of seawater TA contribute negligibly to TA near pH 4.5. Current seawater analysis methods call for titration at lower pH (3.5–3.0; Dickson et al. 2007). However, with accurate pH measurements, TA can be measured at higher pH, providing results consistent with the formal definition of TA (Liu et al. 2011).

$$\begin{aligned} TA = {} & \left[HCO_3^-\right] + 2\left[CO_3^{-2}\right] + \left[B(OH)_4^-\right] + \left[OH^-\right] + \left[HPO_4^{-2}\right] \\ & + 2\left[PO_4^{-3}\right] + \left[H_3SiO_4^-\right] + 2\left[H_2SiO_4^{-2}\right] + \left[HS^-\right] + 2\left[S^{-2}\right] \\ & + \left[NH_3^0\right] + \left[OrgAlk^-_{pKa \geq 4.5}\right] - \left[H^+\right] - \left[HSO_4^-\right] - [HF] \\ & - [H_3PO_4] - \left[OrgAlk^-_{pKa < 4.5}\right] \end{aligned} \quad (2)$$

However, definitions of TA have included a catch-all term of unspecified organic anions ($OrgAlk^-$ terms in Eq. 2, denoted simply as OrgAlk in this work). These organics will contribute to TA in a manner consistent with Eq. 2, provided that they become fully protonated at or above pH 4.5 (i.e., have a pK_a substantially greater than 4.5, termed $[OrgAlk^-_{pKa \geq 4.5}]$ in Eq. 2). However, there is increasing evidence that the acid–base behavior of naturally occurring organic anions is inconsistent with this convention, with some functional groups having a pK_a near or below 4.5 ($[OrgAlk^-_{pKa<4.5}]$ in Eq. 2; Ulfsbo et al. 2015; Sharp and Byrne 2020; Song et al. 2020; Sharp and Byrne 2021; Kerr et al. 2023a).

In this study we sampled two Gulf of Maine estuary systems: the Pleasant estuary in Maine, USA, and the St. John estuary in New Brunswick, CA. Samples were collected along the estuary salinity gradient and at the river endmember over four spring and fall transits. Using two different measurement protocols, these samples were analyzed via titration with base for several parameters including OrgAlk charge group concentrations and pK_a. This work presents the resulting OrgAlk concentrations, modeled estuary organic matter pK_a values and charge group concentrations and examines retrievals of pH using inorganic carbon system calculations.

Materials and methods

Study sites

Based on previous work documenting contrasting levels of dissolved organic carbon (DOC), TA, OrgAlk, and pH measured at several New England and Canadian river endmembers

(Hunt et al. 2011), two river-estuary systems were selected for this study (Fig. 1). The Pleasant river drains an approximately 160 km^2 watershed forested in deciduous trees, but is also characterized by large regions of heath predominantly used to cultivate wild blueberries. Pleasant river water is known to be rich in tannins (a synonym for humic acids), and the darkly colored water empties into the marsh-fringed estuary at the town of Columbia Falls (Keller 2020). The St. John river drains a much larger watershed, approximately 55,000 km^2, which encompasses areas of Maine (USA) and New Brunswick (Canada). The river empties into the Bay of Fundy at St. John, New Brunswick, although vigorous tidal mixing occurs above and below this location. The watershed is mostly forested, with occasional agricultural areas. Soils are loamy and well-drained, overlying a mixture of limestone and sandstone bedrock (Fahmy et al. 2010).

Sample collection

In order to assess potential differences in estuary conditions between spring and fall seasons, four surveys of the Pleasant and St. John estuaries were conducted in May and October of both 2018 and 2019. Estuary samples were collected during single-day surveys on small vessels in each system, departing from Addison Maine for Pleasant estuary surveys and from St. John, New Brunswick, for St. John surveys. Estuary water was continuously pumped to an underway measurement system, which recorded location, salinity, water temperature, and the partial pressure of carbon dioxide (pCO_2) among other parameters. A detailed description of this underway system

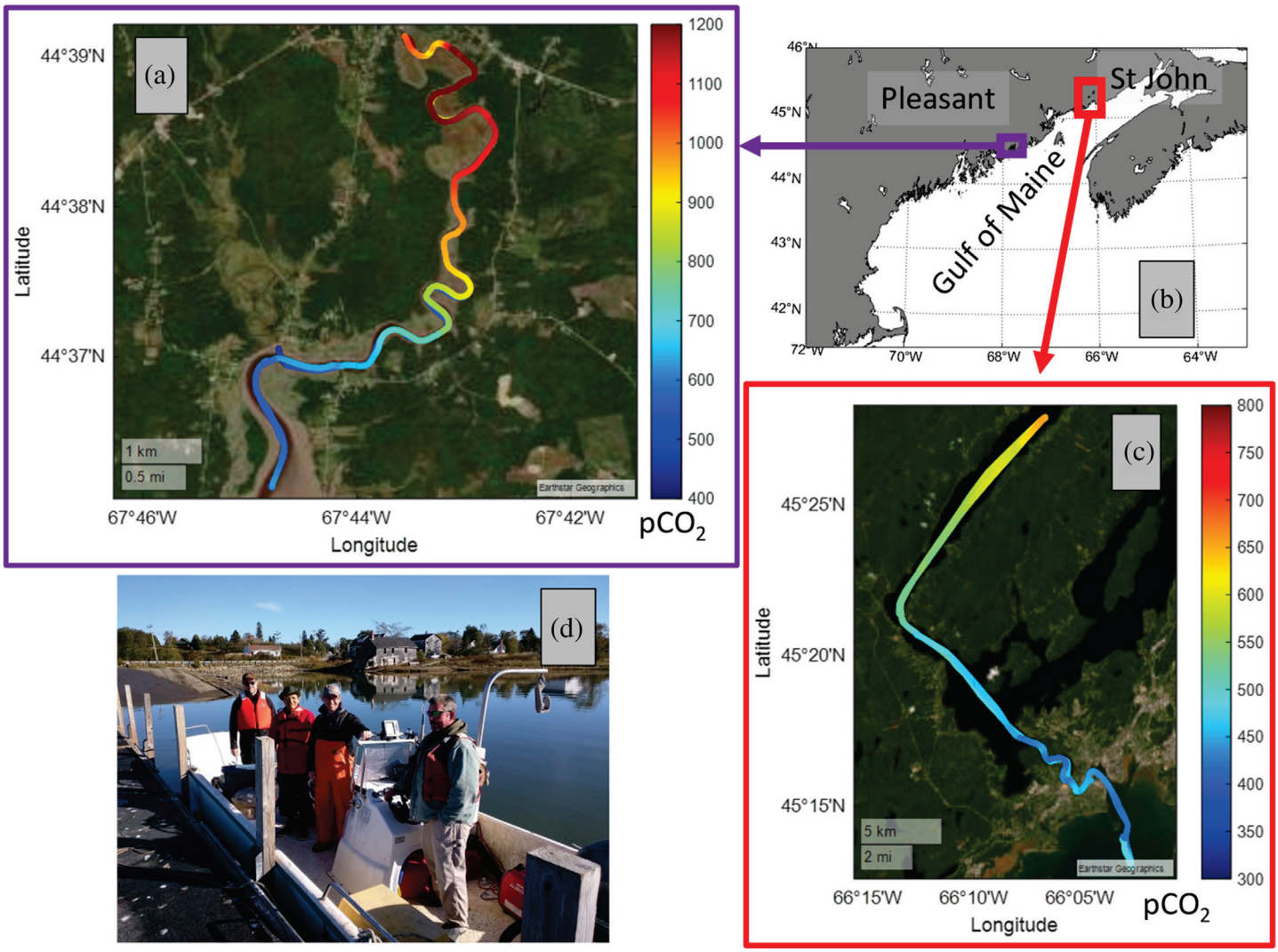

Figure 1. Clockwise from top left: (**a**) The Pleasant estuary with underway vessel track colored by partial pressure of carbon dioxide (pCO_2) observed in October 2018. (**b**) Regional map of the Gulf of Maine with the Pleasant estuary in purple and St John in red. (**c**) The St John estuary with underway ship track colored by pCO_2 observed in October 2018. (**d**) Survey vessel on the Pleasant estuary. Note the different pCO_2 color scales in panels (**a**) and (**c**). Map imagery courtesy of Google.

can be found in Hunt et al. (2013). Surveys began on the incoming tide and lasted through high tide and into the ebb tide. At intervals determined from the underway salinity, surface water was captured for discrete sample collection. During the October 2017 and May 2018 surveys a Niskin bottle was lowered overboard by hand; during the later surveys a 10-L high-density polyethylene carboy was rinsed and filled from the outflow of the underway system, then tightly capped until samples were drawn from a spout at the bottom of the carboy. River endmember samples were collected from above the final downstream dam on each river. For the Pleasant, this dam formed a physical tidal barrier, and the transition from river to estuary was immediate. For the St. John the closest site was in Fredericton New Brunswick, a location over 120 km from the estuary mouth along the river's course. For both endmember sites, a plastic bucket was lowered from the center of a bridge over the river, rinsed three times with river water, and samples were collected as described earlier. The temperature and conductivity of samples were measured directly from the bucket with a handheld meter (YSI).

Water from the Niskin or carboy was transferred without bubbling into individual, previously-flushed borosilicate glass bottles: 500 mL for alkalinity and pH analyses, and 300 mL for inorganic carbon (DIC) analysis. All bottles had greased stoppers and positive closure mechanisms. All were filled to leave less than 1% headspace in the bottle and were preserved with saturated mercuric chloride solution. Samples for silicate and phosphate analysis were filtered using a plastic syringe and 0.2 μm cartridge filter into acid-washed and previously rinsed 50-mL high-density polyethylene vials and preserved with chloroform. Samples for DOC were filtered as was done for the nutrients into acid-washed, previously rinsed 30-mL high-density polyethylene bottles. All samples were immediately placed on ice. Alkalinity, pH (on the total pH scale, pH_T), and DIC samples were refrigerated until analysis; nutrient and DOC samples were frozen until analysis.

Analytical methods

Discrete sample salinity was measured with a Guildline Portasal salinometer (Guildline, Smiths Falls Canada). The pH_T of samples above pH_T 7.0 was measured spectrophotometrically with meta-cresol purple (mCP) using 10 cm pathlength cylindrical glass cells and an Agilent Technologies Cary 8454 UV–Vis spectrometer (estimated pH_T precision: 0.001). Samples measured using mCP ranged in salinity from 0.5 to 32.5 (Douglas and Byrne 2017). The same instrument was used to verify the response slope of a combination glass pH electrode (Metrohm EcoTrode Plus), as described in Supporting Information Section S1. For sample pH_T less than 7.0, and therefore outside the working range of mCP, the initial electrode mV reading and zero-pH_T intercept potential (E_0) determined from the initial TA titration (Alk_{Gran1}, equivalent to TA, *see* Alkalinity titrations section; Easley and Byrne 2012) were used to calculate the pH_T of the untitrated sample. All pH_T measurements were performed on samples preserved with mercuric chloride. The DOC was measured with an uncertainty of 1.5 μmol kg^{-1} using a Shimadzu high temperature catalytic oxidation analyzer with chemiluminescent detection. Nutrients including phosphate and silicate were analyzed using a SmartChem automated analyzer (Westco Scientific) according to standard colorimetric methods. The resulting measurement uncertainties were 0.8 and 0.25 μmol kg^{-1}, respectively (Strickland and Parsons 1972). The DIC was measured by acidifying each sample in a custom-built gas extraction system and measuring the evolved CO_2 with a Picarro G5131-I cavity ringdown spectrometer (Picarro), with an estimated measurement uncertainty of 2 μmol kg^{-1}.

Alkalinity titrations

The TA and OrgAlk titrations were conducted using a custom-built apparatus similar to that presented in Cai et al. (1998). This system performed several successive titrations on the same water sample. The TA of each sample was measured by Gran titration (Alk_{Gran1}) according to an accepted method ("Standard Operating Procedure 3b"; Dickson et al. 2007), followed by measurement of the carbonate-free alkalinity also using the Gran titration approach ($NC\text{-}Alk_{Gran2}$), and finally the carbonate-free alkalinity was measured according to an endpoint approach at pH_T 4.5 ($NC\text{-}Alk_{4.5}$). Details of the analyses are provided in Supporting Information Section S2. Briefly, each sample was initially titrated from the initial pH_T (pH_{Ti}) to a pH_T of 3.5, bubbled with nitrogen, then titrated to pH_T 3.0 (Alk_{Gran1}). CO_2-free NaOH (described in Supporting Information Section S3) was then added to return the sample to an alkaline pH_i. The sample was then titrated to pH_T 3.0 ($NC\text{-}Alk_{Gran2}$). This process was then repeated, with the final titration ending at pH_T 4.5 ($NC\text{-}Alk_{4.5}$). Repeated analyses of certified reference material (CRM; Dickson et al. 2003) produced a mean deviation from CRM alkalinity of -2.1 μmol kg^{-1} with a standard deviation of $\pm$ 5.0 μmol kg^{-1}.

NaOH titrations

We generally followed the methods presented by Cai et al. (1998), Song et al. (2020), and Kerr et al. (2023a) to estimate both organic proton binding site concentrations (XT_i) and corresponding acid dissociation constants (pK_{ai}). Details are provided in Supporting Information Section S4. Briefly, a sample was acidified to pH_T 3.0 via Gran titration (Alk_{Gran1}), then automatically titrated stepwise under nitrogen with small additions of CO_2-free NaOH from pH_T 3.0 to pH_T 8.5 or 10, resulting in several hundred sequential NaOH additions.

Calculation of Alk_{Gran1}, $NC\text{-}Alk_{Gran2}$, and $NC\text{-}Alk_{4.5}$

Alk_{Gran1} and $NC\text{-}Alk_{Gran2}$ were calculated using the Gran function (Gran 1952) that included a nonlinear least squares correction for the presence of sulfate and fluoride ions (Dickson et al. 2007). At an endpoint of 4.5, $NC\text{-}Alk_{4.5}$ was simply determined as the difference between the concentration of added

protons from the HCl titrant and the measured proton concentration:

$$\text{NC-Alk}_{4.5} = \frac{m_A c_A}{m_0} - \frac{[\text{H}^+](m_0 + m_A)}{m_0} \quad (3)$$

where m_A is the mass of added HCl titrant, c_A is the concentration of HCl titrant, m_0 is the initial sample mass, and $[\text{H}^+]$ is the proton concentration determined from the endpoint pH_T measurement. The titration pH_T was calculated from the observed E_0 determined during the $\text{Alk}_{\text{Gran1}}$ measurement for each sample:

$$\text{pH}_\text{T} = \frac{E - E_0}{RT \times \frac{\ln(10)}{F}} \quad (4)$$

where E is the electrode potential (volts) measured at the titration endpoint, E_0 is the electrode intercept potential, R is the gas constant (8.3145 J K^{-1} mol^{-1}), T is the Kelvin temperature of the titration, and F is the Faraday constant (96,487 C mol^{-1}).

Calculation of $\text{OrgAlk}_{\text{Gran2}}$ and $\text{OrgAlk}_{4.5}$

As $\text{NC-Alk}_{\text{Gran2}}$ and $\text{NC-Alk}_{4.5}$ titrations were performed under CO_2-free solutions, their values are represented as the sum contribution of non-carbonate alkalinity components (NC-Alk_x):

$$\begin{aligned}\text{NC-Alk}_x = {} & [\text{OH}^-] + 2[\text{PO}_4^{3-}] + [\text{HPO}_4^{2-}] \\ & + [\text{SiO(OH)}_3^-] + [\text{B(OH)}_4^-] + [\text{OrgAlk}_x] - [\text{H}^+] \end{aligned} \quad (5)$$

where NC-Alk_x is either $\text{NC-Alk}_{\text{Gran2}}$ or $\text{NC-Alk}_{4.5}$. OrgAlk_x represents the contribution of organic species to $\text{NC-Alk}_{\text{Gran2}}$ or $\text{NC-Alk}_{4.5}$. It was calculated as the residual after all other alkalinity species were taken into account. Phosphate and silicate CRM concentrations were both taken from reported CRM documentation. For natural samples they were measured by standard colorimetric methods using a SmartChem automated analyzer (Westco Scientific).

Calculation of pK_{ai} and XT_i from NaOH titrations

Nonlinear least squares fitting of the NaOH titration curve produced estimates of both XT_i (the concentration of organic proton binding group i) and pK_i (the acid dissociation constant of organic proton binding group i). Details of this analysis are provided in the Supporting Information. Briefly, this approach is identical to that of Cai et al. (1998), Song et al. (2020), and Kerr et al. (2023a), with the exceptions that (1) terms used by Song et al. (2020) and Kerr et al. (2023a) to account for excess CO_2 in the NaOH titrant were excluded, and (2) we modeled both the entire NaOH titration curve as was done in other studies, and also subsets of the NaOH titration curve over a more limited range of pH_T.

Calculation of $\sum\text{XT}_i$, XT_{Gran2}

The quantities of $\text{OrgAlk}_{\text{Gran2}}$ and $\sum\text{XT}_i$ are not directly comparable, as $\text{OrgAlk}_{\text{Gran2}}$ only represents the organic anions that are unprotonated at pH_i (i.e., $[\text{Org}^-]$), while $\sum\text{XT}_i$ represents the sum concentrations of i organic charge groups in solution (i.e., $\sum_i [\text{HOrg}_i] + [\text{Org}_i^-]$). To account for this difference, we followed the approach of Song et al. (2020), which uses the OrgAlk measured from pH_i ($\text{OrgAlk}_{\text{Gran2}}$) together with the component fractions of XT_i comprising $\sum\text{XT}_i$ and the dissociation constants (K_i) provided by the NaOH titration, to calculate the total organic proton binding group concentration XT_{Gran2}:

$$\text{OrgAlk}_{\text{Gran2}} = \frac{\frac{\text{XT}_1}{\sum\text{XT}_i} \times \text{XT}_{\text{Gran2}}}{1 + \frac{[\text{H}_\text{i}^+]}{K_1}} + \frac{\frac{\text{XT}_2}{\sum\text{XT}_i} \times \text{XT}_{\text{Gran2}}}{1 + \frac{[\text{H}_i^+]}{K_2}} + \frac{\frac{\text{XT}_3}{\sum\text{XT}_i} \times \text{XT}_{\text{Gran2}}}{1 + \frac{[\text{H}_i^+]}{K_3}} \quad (6)$$

where $[\text{H}_i^+]$ is the hydrogen ion concentration at pH_i, which is the pH_T at which $\text{OrgAlk}_{\text{Gran2}}$ was measured.

Calculation of pH_T from carbonate system parameters

To evaluate the influence of OrgAlk on estuary water chemistry, we chose to examine differences between observed pH_T and those calculated from several combinations of carbonate system parameters ($\text{Alk}_{\text{Gran1}}$, DIC, pCO_2). We used a modified version of CO2SYS (Van Heuven et al. 2017) provided by Song et al. (2023), which accepts the input of the pK_{ai} and charge group concentrations (XT_i) of three OrgAlk groups, together with silicate and phosphate concentrations. The inorganic carbon K_1 and K_2 constants chosen were those of Millero et al. (2010), the K_{SO4} and K_B constants were those of Dickson et al. 1990 and Dickson 1990, respectively, and the total boron concentration was calculated from salinity according to Uppström (1974). A discussion of uncertainty propagation in the pH_T calculations and potential sources of interference is presented in Supporting Information Sections S6 and S7.

Results

The Pleasant endmember was highly acidic and poorly buffered, with a mean pH_T of 4.40 and mean $\text{Alk}_{\text{Gran1}}$ of − 39 μmol kg^{-1} (Table 1). The negative alkalinity concentration relates to a deficit of proton donors relative to proton acceptors; as the equivalence point of TA is defined at pH_T 4.5 (Dickson 1981) a sample with a natural pH_T less than 4.5 is expected to exhibit negative $\text{Alk}_{\text{Gran1}}$. The St. John was more buffered, with a mean pH_T of 6.81 and mean $\text{Alk}_{\text{Gran1}}$ of 650 μmol kg^{-1}. The mean Pleasant endmember DOC (1238 μmol kg^{-1}) was also double that of the St. John (612 μmol kg^{-1}), while the mean St. John DIC was more than four times higher than that of the Pleasant. The October surveys in both systems followed dry summers with low river

Table 1. Endmember characteristics for the four surveys described in this study. Minimum and maximum values are shown, with the mean and one standard deviation in square brackets. Negative values are shown in parentheses.

	Pleasant	St. John	Seawater (salinity > 30)
Alk_{Gran1} (μmol kg^{-1})	(− 92)–(−15) [−39 ± 36]	463–858 [650 ± 182]	2029–2194 [2145 ± 78]
pH_T	3.976–4.785 [4.394 ± 0.333]	6.437–6.920 [6.808 ± 0.356]	7.641–7.755 [7.714 ± 0.05]
DIC (μmol kg^{-1})	123–211 [153 ± 40]	337–978 [691 ± 201]	2050–2136 [2101 ± 45]
DOC (μmol kg^{-1})	545–1944 [1238 ± 720]	463–882 [612 ± 185]	83–128 [99 ± 18]
$OrgAlk_{Gran2}$ (μmol kg^{-1})	(− 31)–(−12) [−25 ± 8.9]	40–51 [43 ± 5.6]	7–30 [16 ± 10]
$OrgAlk_{4.5}$ (μmol kg^{-1})	NA	24–33 [28 ± 3.8]	6–29 [14 ± 10]

Alk_{Gran1}, initial total alkalinity titration; DIC, dissolved inorganic carbon; DOC, dissolved organic carbon; OrgAlk, organic alkalinity.

discharge and coincided with the highest endmember pH_T and Alk_{Gran1}, DIC, and DOC concentrations.

Alk_{Gran1}, pH_T, and DOC distributions with salinity in both the Pleasant and St. John reflected the mixing of the distinct river endmembers with a common Gulf of Maine higher-salinity endmember (Fig. 2). Alk_{Gran1} and pH_T in the Pleasant estuary were consistently lower than the St. John at the same salinity. Alk_{Gran1} in both estuaries reflected mostly conservative mixing across the salinity gradient. However, at salinities less than 3 the Pleasant estuary Alk_{Gran1} exhibited some nonlinear characteristics with lower-than-conservative Alk_{Gran1}.

As pH_T quantifies proton concentrations on a logarithmic scale, nonlinear pH_T distributions with salinity are expected. Although pH_T values below 6 in the Pleasant estuary reflected a strongly acidic system, pH_T was higher by several tenths across the salinity range during May surveys in the Pleasant estuary when compared to October surveys, especially in midrange salinities from 3 to 25. The opposite was true in the St. John estuary, when salinity was lower in May than October. In contrast to Alk_{Gran1} and pH, DOC was consistently higher in the Pleasant estuary than in the St John at a comparable salinity and season. While St. John DOC-salinity distributions were similar across the four surveys, with the possible exception of the October 2019 St. John survey, DOC concentrations across the Pleasant estuary salinity gradient in October were more than twice as high as those in May (Fig. 2).

Estuary OrgAlk

Organic alkalinity, measured as $OrgAlk_{Gran2}$ and $OrgAlk_{4.5}$, was observed in both the Pleasant and St. John estuaries in all four surveys (Fig. 3, Table 1). As with Alk_{Gran1}, the Pleasant endmember $OrgAlk_{Gran2}$ was consistently negative, reflecting the low pH_T conditions of the Pleasant River. This low pH_T did not permit the measurement of $OrgAlk_{4.5}$. The St. John low-salinity endmember had consistent $OrgAlk_{Gran2}$ and $OrgAlk_{4.5}$ concentrations, with mean values of 43 ± 5.6 and 28 ± 3.8 μmol kg^{-1}, respectively. Estuarine mixing rapidly changed the distributions of $OrgAlk_{Gran2}$ and $OrgAlk_{4.5}$ in the Pleasant estuary, with increasing salinity coinciding with $OrgAlk_{Gran2}$ and $OrgAlk_{4.5}$ increasing to mid-estuary maxima and then decreasing towards the ocean endmember. This low-salinity increase was particularly large in the Pleasant October surveys, when $OrgAlk_{Gran2}$ rose more than 100 μmol kg^{-1}. $OrgAlk_{Gran2}$ and $OrgAlk_{4.5}$ were typically higher in the Pleasant estuary than in the St. John above a salinity of 3 in the October surveys, while concentrations were similar between the two systems during the May surveys. Maximum $OrgAlk_{Gran2}$ and $OrgAlk_{4.5}$ concentrations were typically found between salinities 1–11, with exceptions in the Pleasant estuary in May 2018 where the maximum values were at higher salinities, and the St. John in October 2018 when the maximum $OrgAlk_{4.5}$ was found at the highest salinity (32.10). $OrgAlk_{Gran2}$ concentrations were consistently higher than the respective $OrgAlk_{4.5}$ concentrations at low and middle estuary salinity, but the concentrations typically became comparable at salinities above 25. OrgAlk can also be estimated as the difference between titrated TA and TA calculated from other carbonate system parameters (e.g., pCO_2 and DIC; Hunt et al. 2011; Ko et al. 2016; Song et al. 2020). However, a comparison of Pleasant and St. John estuary titrated $OrgAlk_{Gran2}$ results to OrgAlk calculated according to this difference approach (using pCO_2 and DIC to estimate TA) found no correspondence ($p > 0.08$, $r^2 = 0.04$, data not shown). Song et al. (2020) also found no correlation between these two OrgAlk measures.

Whole-pH titration results ($\sum XT_i$, pK_a)

Modeling of the NaOH titration data resulted in consistent pK_a values for OrgAlk (Table 2). Three organic proton binding groups were returned by the model when all titration data were used, with overall mean pK_a values of 4.16 (± 0.35), 5.93 (± 0.50), and 8.49 (± 0.21). While the discussion focuses on these results, it is worth noting that modeling NaOH titration data between pH_T 3.0 and sample in situ (pH_i) produced either two or three groups, indicating that the pH_T range of data modeled impacted the model output. There was no statistical difference between mean pK_a in the Pleasant and St. John estuaries, and there were no seasonal differences between May and October pK_a for either estuary.

Analysis of NaOH titration data also produced organic charge group concentrations (XT_i) for the three selected

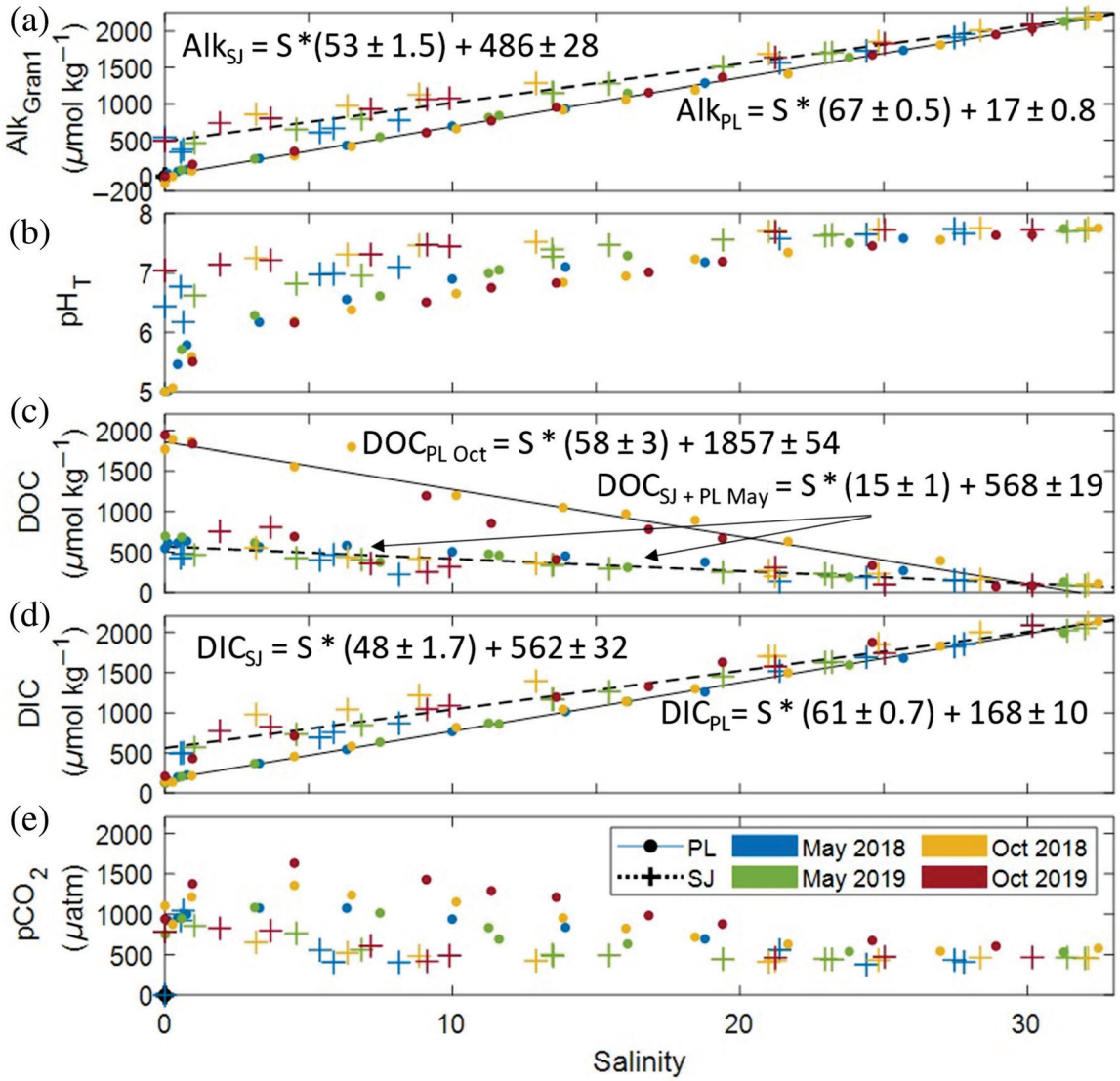

Figure 2. Distributions against salinity in the Pleasant (circles) and St. John (crosses) estuaries, from top to bottom, of (**a**) initial total alkalinity titration (Alk_{Gran1}) (μmol kg^{-1}), (**b**) pH_T (total scale), (**c**) dissolved organic carbon (μmol kg^{-1}), (**d**) dissolved inorganic carbon (DIC) (μmol kg^{-1}), and (**e**) partial pressure of carbon dioxide (pCO_2) (μatm). Linear regression lines for all seasons are shown for Alk_{Gran1} and DIC in the Pleasant (solid lines) and St. John (dashed lines). Note that the solid linear regression line for dissolved organic carbon (DOC) shows data for the Pleasant estuary in October, while the dashed DOC line shows combined data for the Pleasant estuary in May and all St. John estuary data (also indicated by arrows in panel **c**). The root mean square error (RMSE) for the regression lines was Alk_{SJ} = 101, Alk_{PL} = 36, DOC_{PL} Oct = 157, $DOC_{SJ+PLMay}$ = 84, DIC_{SJ} = 105, and DIC_{PL} = 41 (all in μmol kg^{-1}).

organic proton binding groups (*see* Supporting Information Section S4). Concentrations of XT_3 (mean pK_{a3} 8.49) were always greatest, typically followed by XT_1 (mean pK_{a1} 4.16), and XT_2 (mean pK_{a2} 5.93). The total concentration of all organic charge groups ($\sum XT_i = XT_1 + XT_2 + XT_3$; Fig. 4) ranged from 158 μmol kg^{-1} in the highest-salinity Pleasant estuary sample in May 2019 to 1350 μmol kg^{-1} in the Pleasant estuary in Oct. 2018. The mean $\sum XT_i$ for all samples in both estuaries was 361 μmol kg^{-1} ($\pm$ 194 μmol kg^{-1}). The proportional contribution of each group to $\sum XT_i$ was consistent: 21% ± 9% XT_1 (range: 1%–54%), 8% ± 5% XT_2 (range 0%–24%) and 71% ± 11% XT_3 (range 33%–93%).

Titrated organic proton binding group concentrations (XT_{Gran2})

XT_{Gran2} was almost always lower than respective $\sum XT_i$ (Fig. 4), and neither showed any trend with salinity. Note that negative values of $OrgAlk_{Gran2}$ returned negative values of XT_{Gran2} according to Eq. 6. As a negative total concentration is not possible (unlike a negative alkalinity defined relative to a proton equivalence point), we have ignored these values in

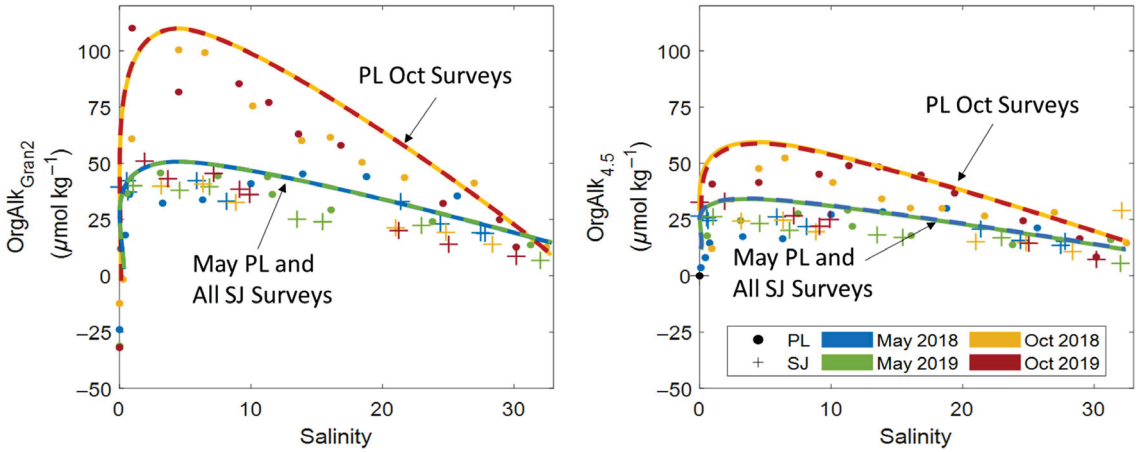

Figure 3. Distributions of $OrgAlk_{Gran2}$ (left column, μmol kg^{-1}) and $OrgAlk_{4.5}$ (right column, μmol kg^{-1}) plotted against salinity in the Pleasant and St. John estuaries. Lines are intended as a qualitative guide to the eye. Red/orange lines are drawn to show the distribution of Pleasant estuary OrgAlk data during October surveys, while blue/green lines show the distribution of all St. John estuary and May Pleasant estuary OrgAlk data. OrgAlk, organic alkalinity.

the following analysis. The mean XT_{Gran2} for all samples was 136 μmol kg^{-1} ($\pm$ 133 μmol kg^{-1}), with a maximum and minimum of 510 and 16 μmol kg^{-1}, respectively. Overall, Pleasant estuary XT_{Gran2} was not statistically different from St. John estuary XT_{Gran2} (two-sample t-test, $p = 0.36$), and there were no seasonal differences ($p = 0.11$).

Discussion

OrgAlk distributions

Organic alkalinity was present in both the Pleasant and St. John endmembers and estuary samples during all surveys. Indeed, measurable concentrations of OrgAlk were present in CRM as well, confirming findings reported by Sharp and Byrne (2021). Those authors described a method similar to our $OrgAlk_{4.5}$ measurement, and CRM OrgAlk concentrations (10.5, 10.9, and 7.6 μmol kg^{-1} for Batches 172, 176, and 183, respectively, applying the boron : salinity ratio of Uppström 1974) comparable to the concentration we measured in Batch 185 (5.2 μmol kg^{-1}, applying the Uppström ratio). Details of the OrgAlk method evaluation and CRM results are presented in Supporting Information Section S3. The ubiquitous presence of OrgAlk in natural waters from terrestrial to marine systems requires an understanding of the concentrations and chemical nature of this material if TA measurements are to be accurately used in carbon system calculations (Sharp and Byrne 2020).

Concentrations of $OrgAlk_{Gran2}$ and $OrgAlk_{4.5}$ in the Pleasant and St. John estuaries were comparable to those reported in other studies (Fig. 3, Table 3), although the negative $OrgAlk_{Gran2}$ values in the Pleasant are the larger than previously reported. Pleasant estuary $OrgAlk_{Gran2}$ levels and distributions with salinity during October surveys were similar to those reported for the Satilla estuary by Cai et al. (1998), whose analytical approach was used for the $OrgAlk_{Gran2}$ measurements in this study and whose surveys of the Georgian estuary were also conducted in October. The Satilla zero-salinity endmember also had a very high DOC concentration (about 2170 μmol kg^{-1}) resembling the Pleasant river endmember DOC concentrations (1767 and 1944 μmol kg^{-1} in October 2018 and 2019, respectively). Kuliński et al. (2014) also measured very high OrgAlk concentrations in two Baltic rivers, the Oder (184 μmol kg^{-1} OrgAlk) and Vistula (265 μmol kg^{-1} OrgAlk). The DOC concentrations in these Baltic rivers (505 and 614 μmol kg^{-1} DOC, respectively) were lower than the Satilla or Pleasant in October but were quite similar to the Pleasant River DOC concentrations in May (545 and 695 μmol kg^{-1} in May 2018 and 2019, respectively) and St. John endmember DOC concentrations overall. The Oder and Vistula both had much higher TA (2563 and 3366 μmol kg^{-1}, respectively) than the Satilla, Pleasant, or St. John rivers. While the Satilla estuary pH shown in Cai et al. (1998) was not as low as our Pleasant endmember observations, the Satilla pH did approach 5.5 (on the National Bureau of Standards- NBS- scale) at the endmember, the lowest level registered among the studies presented in Table 3.

The Altamaha estuary presented by Cai et al. (1998) most closely resembled the conditions we observed in the St. John, with comparable $OrgAlk_{Gran2}$ (about 5–50 μmol kg^{-1}), DOC concentrations (about 350–750 μmol kg^{-1}), and pH and Alk_{Gran1} near the river endmember (about 6.6 on the NBS scale and 500 μmol kg^{-1}, respectively). The Alk_{Gran1} and pH at the Baltic sites of Kuliński et al. (2014) were much higher than those in the St. John, with lower DOC concentrations as well. Overall, the Satilla estuary is the closest analogue to the Pleasant estuary, while the Altamaha is the closest analogue to the St. John estuary among the systems described in the literature.

Table 2. Aquatic pK_a values determined by several studies.

Sample type	Reported pK_a	Authors
Soil porewater 1	5.3–5.88	Badr et al. (2012)
Soil porewater 2	5.1–5.75	
Soil porewater 3	4.9–5.2	
Sewage sludge	5.25–6.45	
Nile water hyacinth compost	6.5–6.75	
Soil humics	4.28	Andjelkovic et al. (2006)
Adirondack soil/stream humics	3.85	Cronan and Aiken (1985)
Humics	4	Lozovik (2005)
Bickford (MA) watershed	3.5–3.7	Eshleman and Hemond (1985)
River fulvic acid group I	2.66	Paxéus and Wedborg (1985)
River fulvic acid group II	4.21	
River fulvic acid group III	5.35	
River fulvic acid group IV	6.65	
River fulvic acid group V	8.11	
River fulvic acid group VI	9.54	
Satilla estuary group I	4.46	Cai et al. (1998)
Satilla estuary group II	6.64	
Satilla estuary group III	8.94	
Altamaha estuary	6.7	
Savannah estuary	7.1	
Intertidal salt marsh group I	4.1–5.5	Song et al. (2020)
Intertidal salt marsh group II	7.4–9.8	
Baltic Sea	7.53	Kuliński et al. (2014)
Baltic Sea	7.27	Hammer et al. (2017)
Tampa Bay coastal waters	5.31, 7.05	Yang et al. (2015)
Tampa Bay coastal waters	5.45, 7.32	Yang et al. (2015)
Dublin Bay group 1	4.54 (± 0.09)	Kerr et al. (2023a)
Dublin Bay group 2	6.96 (± 0.40)	
Rogerstown Estuary group 1	4.84 (± 0.28)	Kerr et al. (2023b)
Rogerstown Estuary group 2	6.95 (± 0.43)	
Hillsborough River group 1	4.1–6.1	Martell-Bonet and Byrne (2023)
Hillsborough River group 2	6.33 (± 0.01)	
Hillsborough River group 3	8.56–9.32	
Six Chinese estuaries group 1	2.8–3.0	Song et al. (2023)
Six Chinese estuaries group 2	4.4–6.8	
Six Chinese estuaries group 3	6.6–9.6	
Pleasant estuary group 1	4.16 (± 0.35)	This study
Pleasant estuary group 2	5.93 (± 0.50)	
Pleasant estuary group 3	8.49 (± 0.21)	
St. John estuary group 1	4.18 (± 0.70)	
St. John estuary group 2	5.83 (± 0.89)	
St. John estuary group 3	8.51 (± 0.10)	

Middle-estuary OrgAlk maxima

The low-salinity region of estuary mixing is typically the site of dramatic pH increases, particularly in the acidic Pleasant system. Organic alkalinity mixing in the Pleasant estuary surveys also resulted in $OrgAlk_{Gran2}$ and $OrgAlk_{4.5}$ peaks in the middle of the salinity gradient. Cai et al. (1998) documented similar mid-estuary OrgAlk maxima and attributed the phenomenon to two different processes: rapid pH change in early estuary mixing followed by conservative mixing of organic alkalinity between the peak and the coastal endmember. If charge groups with sufficiently low pK_a are present in the organic material, the rapid pH increase results in those groups being increasingly deprotonated at ambient pH and thus available for titration with acid. Cai et al. (1998) theorized that this pH change is of more importance to estuary OrgAlk contributions than the potential dependence of organic pK_a on ionic strength (i.e., salinity). Others have pointed out that salt marshes and mangroves may represent inputs of alkalinity to estuaries, presumably including organic components, independent of river and ocean endmembers (Sippo et al. 2016; Wang et al. 2016), and this could explain the mid-estuary maxima in our observations. Song et al. (2020) proposed a large intertidal salt marsh OrgAlk contribution, representing 36% of the total OrgAlk concentration, during a time of limited freshwater input. However, recent work by Hinckley (2021) provides a counter-argument. Hinckley (2021) serially diluted Pleasant and St. John river water with CRM to artificially simulate the estuary mixing process. These dilutions and titrations effectively removed the low-salinity pH change noted by Cai et al. (1998), but still showed a mid-salinity peak of $OrgAlk_{Gran2}$ and $OrgAlk_{4.5}$. As the only changes among the dilutions were the ionic strength and OrgAlk concentration, the pK_a dependence of organic charge sites on ionic strength may need to be re-evaluated, and may be more important than previously reported.

Differences between $OrgAlk_{Gran2}$ and $OrgAlk_{4.5}$

We measured OrgAlk using two different approaches: a Gran-style interpretation of titration data between pH_T 3.5–3.0, and a separate endpoint titration to the TA equivalence pH_T of 4.5. If no OrgAlk was present in solution, or if the organic charge groups had pK_a values considerably higher than 4.5 or lower than 3.0 (and thus became totally protonated or remained deprotonated during both titration procedures, respectively) then the concentrations of $OrgAlk_{Gran2}$ and $OrgAlk_{4.5}$ would in principle be equal. Alkalinity titrations to different endpoints can be conducted reproducibly, represent the "correct" alkalinity quantity at that particular pH, and provide different overall alkalinities. Our work shows that these differences can be substantial. Organic anions may have a pK_a that impacts the titration alkalinity, but which would not affect buffering or the overall acid–base chemistry at typical estuarine or ocean in situ pH, and careful consider-

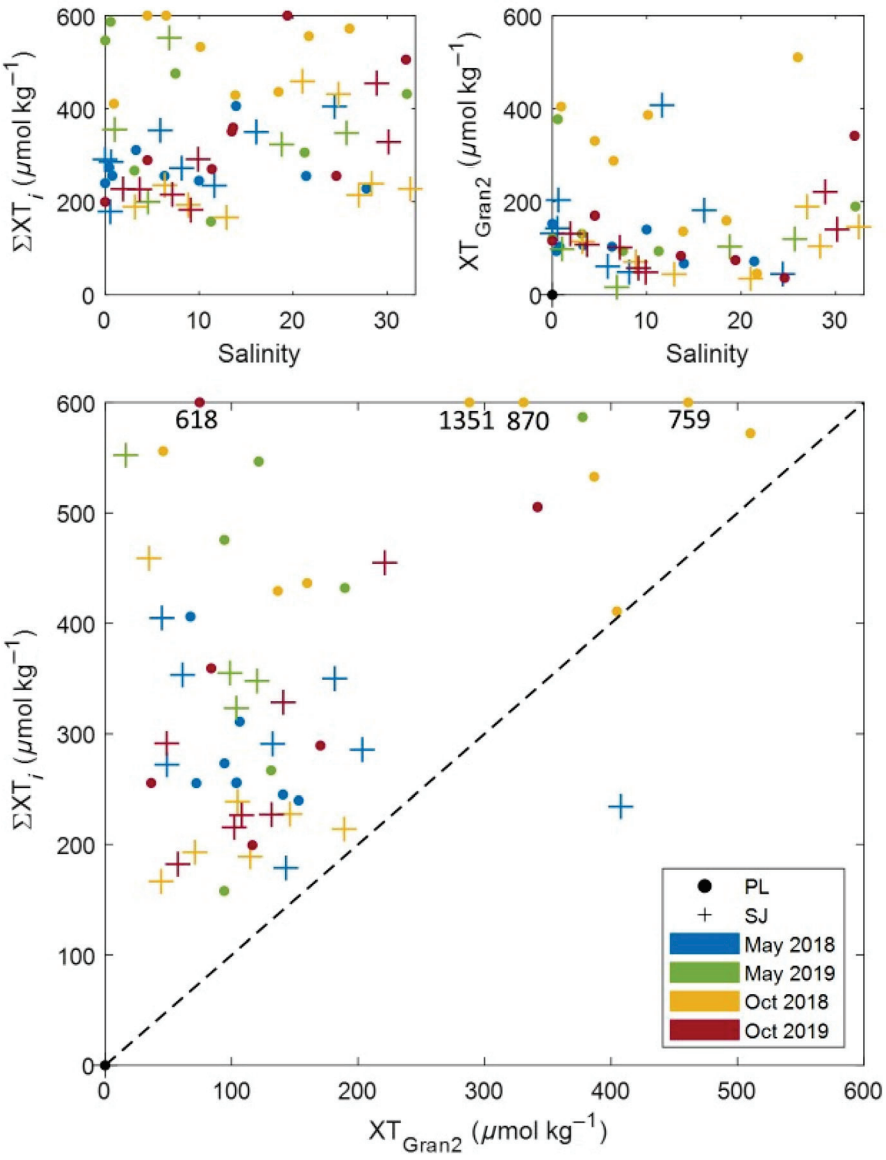

Figure 4. Distributions of $\sum XT_i$ (top left, μmol kg^{-1}) and XT_{Gran2} (top right, μmol kg^{-1}) in the Pleasant and St. John estuaries plotted against salinity and colored by survey month (legend in bottom panel). The bottom plot shows the correspondence between $\sum XT_i$ and XT_{Gran2} with the dashed line being a 1 : 1 trend. Note that values of $\sum XT_i$ greater than 600 μmol kg^{-1} are plotted at the top of the *y*-axis with actual values given immediately below each point. XT_i, organic proton binding site concentration.

ation is required when measuring OrgAlk and discussing its contribution to TA. Indeed, there does not currently appear to be a rigorous means of including OrgAlk in a quantitative summation of all contributions to alkalinity.

While models that included additional charge groups did not appreciably improve modeled Org-Alk fits to our observations, this does not imply that the organic charge groups present in the Pleasant and St John estuaries are actually uniform in their properties. Instead, it is likely that the organic charge groups are polydisperse with a number of distinct pK_a values, as described by Paxéus and Wedborg (1985) and Cai et al. (1998). The simple model and dataset conditions we employed, which only encompassed the natural pH conditions of the Pleasant and St. John estuaries, could not account for charge groups with very low pK_a, such as the pK_a 2.66 group that was listed by Paxéus and Wedborg (1985) as the most abundant organic charge group in their sample. A charge group with pK_a near this value, together with differences in dissociation behavior among higher pK_a charge groups as discussed earlier, could account for discrepancies between our $OrgAlk_{Gran2}$ and $OrgAlk_{4.5}$ observations.

Distributions of XT_{Gran2}, $\sum XT_i$, and DOC

$\sum XT_i$ was generally greater than comparable XT_{Gran2} (Fig. 4), and both were generally more variable in the Pleasant

Table 3. Organic alkalinity ranges reported by several studies in estuary or coastal ocean systems, the range of salinity ("nr" indicating the salinity was not reported) in each study, the method of organic alkalinity (OrgAlk) determination, and the referring study. The Gran2 and Endpoint 4.5 methods correspond to those described in this work, while the $\Delta OrgAlk_{(TA,DIC,pH)}$ method employed measurements of total alkalinity, dissolved inorganic carbon, and pH, together with calculated dissociation constants, to overdetermine the carbonate system and calculate OrgAlk. Negative values are shown in parentheses.

System	OrgAlk minimum (μmol kg^{-1})	OrgAlk maximum (μmol kg^{-1})	Salinity range	Method	Study
Satilla estuary	25	115	0–27	Gran2	Cai et al. (1998)
Altamaha estuary	10	50	0–32	Gran2	Cai et al. (1998)
Savannah estuary	20	40	0–25	Gran2	Cai et al. (1998)
Baltic Sea	22	58	3–8	$\Delta OrgAlk_{(TA,DIC,pH)}$	Kuliński et al. (2014)
N. Gulf California	0	120	nr	$\Delta OrgAlk_{(TA,DIC,pH)}$	Hernández-Ayon et al. (2007)
San Diego Bay	100	200	nr	$\Delta OrgAlk_{(TA,DIC,pH)}$	Hernández-Ayon et al. (2007)
San Quintin Bay	0	70	nr	$\Delta OrgAlk_{(TA,DIC,pH)}$	Hernández-Ayon et al. (2007)
Gulf of Mexico/Florida	(−19)	90	20–38	$\Delta OrgAlk_{(TA,DIC,pH)}$	Yang et al. (2015)
Gulf of Mexico/Florida	0	40	22–33	Spectrophotometric titration	Yang et al. (2015)
Baltic Sea	(−8)	50	7–14	$\Delta OrgAlk_{(TA,DIC,pH)}$	Hammer et al. (2017)
Waquoit Bay, Massachusetts	20	80	22–31	Gran2	Song et al. (2020)
Six Chinese estuaries	5	65	0–35	Gran2	Song et al. (2023)
Dublin Bay	50	230	0–36	Gran2	Kerr et al. (2023a)
Rogerstown estuary	40	200	25–33	Gran2	Kerr et al. (2023b)
Pleasant estuary $OrgAlk_{Gran2}$	(−31.9)	110	0–32	Gran2	This study
Pleasant estuary $OrgAlk_{4.5}$	4	52	0–32	Endpoint 4.5	This study
St. John estuary $OrgAlk_{Gran2}$	7	51	1–30	Gran2	This study
St. John estuary $OrgAlk_{4.5}$	6	55	1–30	Endpoint 4.5	This study

than the St. John. Differences between $\sum XT_i$ and XT_{Gran2} may have a number of origins but could be related to the hysteresis between HCl and NaOH titrations of organic material observed by Paxéus and Wedborg (1985). Similar titrations of the same estuary sample in this study using both HCl and NaOH titrants should produce similar hysteresis in the titration curves. Unlike $OrgAlk_{Gran2}$ and $OrgAlk_{4.5}$, $\sum XT_i$ and XT_{Gran2} had no correspondence with salinity or season (Fig. 4). The same lack of correspondence was found with organic charge groups 1–3 (Supporting Information). Additionally, $\sum XT_i$ and $XT_{i,Gran2}$ did not covary with DOC concentrations (Figs. 2, 4). The DOC concentrations along the salinity gradient were consistent among the St. John surveys but demonstrated a clear seasonal shift in the Pleasant estuary, with much higher DOC concentrations at low salinity during the October surveys in comparison to the May surveys (Fig. 2). The Pleasant October surveys were conducted after months of very low precipitation and river flow, which may have resulted in Pleasant river water being comprised of surface runoff, soil porewater, or groundwater that was enhanced in DOC. These higher DOC concentrations were also reflected in the generally higher measured Pleasant estuary $OrgAlk_{Gran2}$ and $OrgAlk_{4.5}$ (Fig. 3).

Alkalinity measured during the NaOH or $OrgAlk_{Gran2}$ titrations and not attributable to inorganic species is presumably associated with organic charge groups, which should be found in proportion to DOC. But while DOC concentrations generally decreased with increasing salinity, indicating a terrestrial source, $\sum XT_i$ and XT_{Gran2} either increased or remained approximately constant with increasing salinity. This agrees with Song et al. (2023), who found greater OrgAlk calculated from $\sum XT_i$ and pK_{ai} than $OrgAlk_{Gran2}$, and greater seaward $\sum XT_i$ than river $\sum XT_i$ in four of six studied estuaries. These authors attributed this difference to the omission of ionic strength in the charge balance model used to determine $\sum XT_i$ and pK_{ai}. Kerr et al. (2023b) also documented a lack of $\sum XT_i$ variability across a salinity gradient for charge Group 1 ($pK_a \sim 4.8$), although charge Group 2 ($pK_a \sim 6.9$) did show a more distinct decrease with increasing salinity. These authors suggested tidally driven sediment resuspension may contribute to the addition of organic material, but our DOC results do not show higher DOC led to an addition of $\sum XT_i$ or XT_{Gran2}. It seems apparent that factors apart from the mixing of high-DOC river water and lower-DOC coastal water are responsible for the distributions or perhaps availability of $\sum XT_i$ or XT_{Gran2}, and that new analytical methods are needed to better understand the sources and characteristics of organic charge groups. Molecular separation approaches may offer a way to examine the alkalinity contributions and characteristics of broad classes of organics such as humics and fulvics. A new series of dilution experiments using simple organic acids or organic-rich river water (Hinckley 2021) may illuminate

changes in alkalinity characteristics with changes in ionic strength. These could be coupled with advanced analytical chemistry techniques such as mass spectrometry to examine possible changes in molecular structure along the estuarine gradient. More broadly, a set of analytical best practices is needed in this field bridging inorganic and organic chemical systems. This would allow for better intercomparison of results and less upfront analytical development for researchers new to this topic.

Application of OrgAlk pK_a and XT_{Gran2} or $\sum XT_i$ to pH_T estimation

One way to assess the success of OrgAlk characterization is to incorporate OrgAlk concentrations and pK_a values into carbonate system calculations. If OrgAlk is well characterized, calculated pH_T should match measured pH_T. The pairing of strictly inorganic parameters (DIC and pCO_2) resulted in overestimated pH_T in the low and mid salinity estuary regions of both the Pleasant and St. John estuaries (Fig. 5). The DIC and pCO_2 pairing should reflect the influences of inorganic and organic buffers on both the measured pH_T and measured equilibrium pCO_2. The pH_T overestimates from input DIC and pCO_2 values were sometimes very large (greater than 2 pH units), particularly in the acidic and organic-rich Pleasant estuary. Pairing Alk_{Gran1} with DIC or pCO_2—with no effort to account for OrgAlk—improved pH_T retrievals, particularly at low salinity. However, pH_T discrepancies larger than 0.50 remained, reinforcing the contention that a portion of titrated alkalinity was not attributable to inorganic carbon, and this affected pH_T in a manner that was not reflected by CO2SYS. Including modeled pK_a values for each sample and XT_{Gran2} charge group concentrations slightly improved pH_T retrievals when Alk_{Gran1} was paired with pCO_2 (Fig. 5), but moved calculated pH_T from Alk_{Gran1} and DIC further from observed levels. Finally, substituting $\sum XT_i$ for XT_{Gran2} resulted in the best pH_T retrievals when Alk_{Gran1} was paired with pCO_2, but worse retrievals for Alk_{Gran1} paired with DIC. Lower-pH_T Pleasant samples showed more change in calculated pH_T with the inclusion of OrgAlk when compared to higher pH_T Pleasant samples and St. John samples (Fig. 5). This reinforces the relative importance of inorganic buffering compared to OrgAlk buffering in the two study systems (Supporting Information Section S8, Figs. S4, S5). In the Pleasant sample the in-situ pH_T is more strongly buffered by OrgAlk Groups 1 and 2, resulting

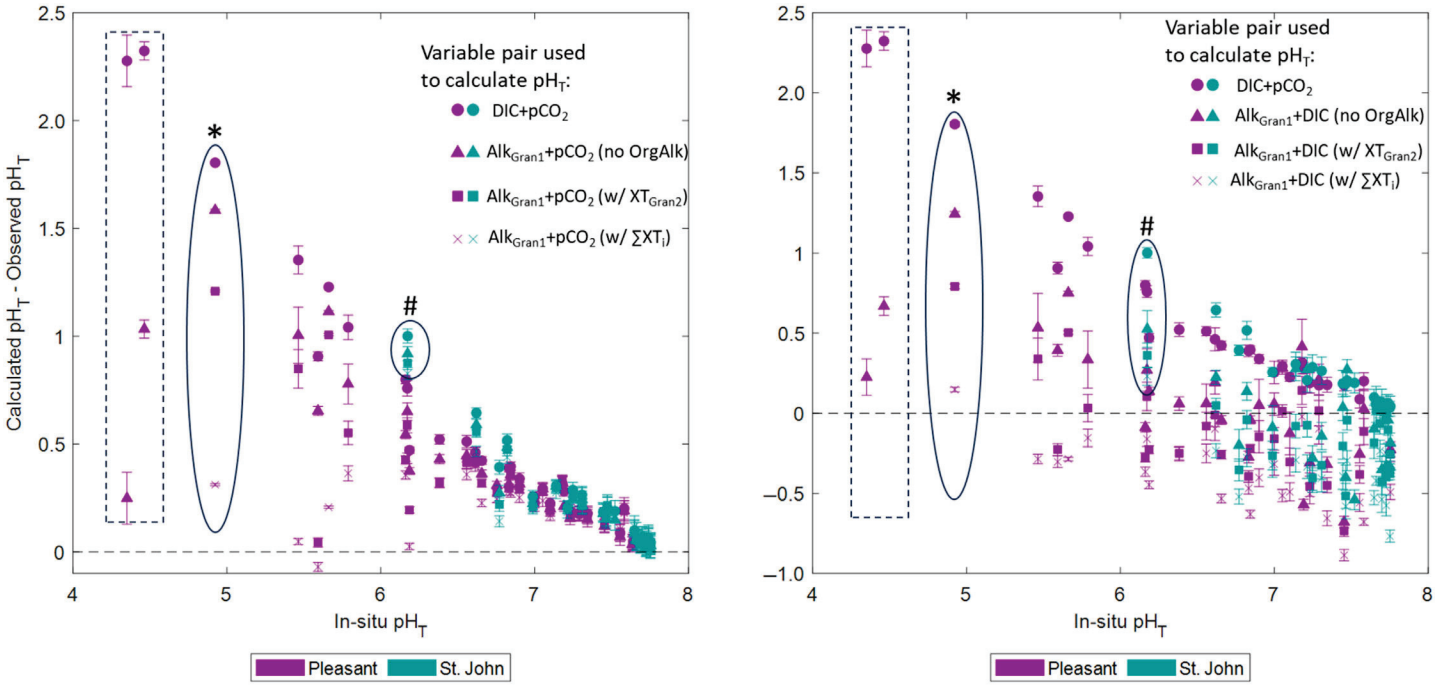

Figure 5. Offsets between observed and calculated pH_T (*y*-axis) plotted against observed pH_T (*x*-axis) in the Pleasant (purple) and St. John (teal) estuaries. Markers indicate the pH_T offsets produced by different input variable pairs (*see* legend at top right). Offsets in the left panel were calculated using input variables of: dissolved inorganic carbon (DIC) and partial pressure of carbon dioxide (pCO_2), initial total alkalinity titration (Alk_{Gran1}) and pCO_2 with no organic alkalinity ("no OrgAlk"), Alk_{Gran1} and pCO_2 with organic alkalinity from Gran2 titrations, ("w/ XT_{Gran2}"), and Alk_{Gran1} and pCO_2 with organic alkalinity from NaOH titrations ("w/ $\sum XT_i$"). Offsets in the right panel were calculated using input variables of: DIC and pCO_2, Alk_{Gran1}, and DIC with no organic alkalinity ("no OrgAlk"), Alk_{Gran1} and DIC with organic alkalinity from Gran2 titrations, ("w/ XT_{Gran2}"), and Alk_{Gran1} and DIC with organic alkalinity from NaOH titrations ("w/ $\sum XT_i$"). Samples circled and marked with "*" and "#" correspond to the data shown in Figs. S2 and S3. Error bars represent the propagated uncertainty of calculated pH_T for each sample according to the "High" uncertainties listed in Supporting Information Table S1. The two samples enclosed by the dashed-line box were analyzed before the XT_{Gran2} and $\sum XT_i$ methods were finalized, thus there are no corresponding pH_T offset values for TA (with XT_{Gran2}) or TA (with $\sum XT_i$). TA, total alkalinity; XT_i, organic proton binding site concentration.

in better calculated pH_T when OrgAlk is included. In the St. John the in situ pH_T is in almost perfect agreement with $pK1_{DIC}$, leading to strong DIC buffering at the in situ pH_T and little effect of OrgAlk on calculated pH_T.

It is worth noting that the Song et al. (2023) version of CO2SYS used in this work does not accept an alkalinity equivalence point input. All organic charge groups given as inputs are treated as proton acceptors (or positive terms in Eq. 2). This approach accounts for all organic proton acceptors that contribute to the observed titration alkalinity. As discussed by Kerr et al. (2023b) this approach is potentially problematic, since the Group 1 pK_a is close to the 4.5 equivalence point defined by Dickson (1981). The 4.5 equivalence point dictates that Group 1 charge groups with a pK_a above 4.5 are proton acceptors, while those with pK_a below 4.5 are proton donors. Thus, most Group 1 charge groups measured in this study should have been apportioned as proton donors (or negative terms in Eq. 2). Given the heterogeneous nature of organic charge groups, the concept of an OrgAlk equivalence point and its application to titration data at pH_T lower than 4.5 needs further examination.

The observation that pairing DIC and pCO_2 produced the largest bias in calculated pH_T, especially in organic-rich waters at low pH, indicates substantial uncertainties in some aspect of either our measurements or carbonate system calculations. We followed standard ocean best practices for all measurements (*see* Methods section and Supporting Information), with resulting low estimated uncertainties. We also performed carbonate system calculations that duplicated the approaches and dissociation constants used in other studies. These analytical and carbonate system calculations may merit re-examination in nearshore and estuary settings. Although inclusion of OrgAlk in pH_T retrieval calculations resulted in some substantial improvements, the persistent and sizeable pH_T offsets that remained illustrate the challenge of carbonate system measurements and calculations in organic-rich estuary systems.

Conclusions

We present some of the first seasonal observations of estuary OrgAlk distributions, measured by different analytic approaches, from two estuaries with contrasting river endmember chemistries. OrgAlk constituted a major part of TA at lower salinities in both estuaries and was an appreciable alkalinity contributor both at higher salinities and in CRM. Distributions of OrgAlk and DOC with salinity varied seasonally in the Pleasant estuary but were seasonally consistent in the St. John estuary. Incremental titrations with NaOH allowed for the estimation of organic acid dissociation constants (pK_a) and total organic charge group concentrations (XT_{Gran2} and $\sum XT_i$). Values of pK_a were quite consistent among seasons and between estuaries, and were in general agreement with other studies. Synthesis of measurements of organic pK_a values may result in a generalized estimate across systems. However, distributions of XT_{Gran2} and $\sum XT_i$ did not show an appreciable trend with salinity, estuary, or season. Paired XT_{Gran2} and $\sum XT_i$ measurements of the same samples also showed a lack of correspondence. Application of XT_{Gran2} and $\sum XT_i$, together with pK_a values, did not fully explain differences between observed and calculated pH_T. The unexplained differences in observed and calculated pH_T indicate that analytical methods and carbonate calculations remain challenging in organic-rich estuary systems, and that our understanding of the titration behavior of organic matter is incomplete. Future studies should take a more fundamental approach, by conducting controlled laboratory experiments in which solutions of simple organic acids are mixed with seawater of known composition. These mixtures could be analyzed following the approaches in this work to examine potential changes in titration behavior with salinity. Once the titration behavior of simple organic acids is shown to be predictable, more complex standard organic acids from natural sources could be tested in the same manner. Additionally, the mixed samples could be analyzed using novel methods, such as the optical methods described by Kerr et al. (2023b) or sophisticated molecular characterization techniques such as Fourier transform ion cyclotron resonance mass spectrometry. Finally, a collaborative effort to standardize OrgAlk measurement methods among laboratories is needed for better intercomparison of results.

Data availability statement

Data and supporting material are available on NSF BCO-DMO: https://www.bco-dmo.org/project/876891.

References

Abril, G., and others. 2014. Technical note: Large overestimation of pCO_2 calculated from pH and alkalinity in acidic, organic-rich freshwaters. Biogeosci. Discuss. **11**: 11701–11725.

Andjelkovic, T., J. Perovic, M. Purenovic, S. Blagojevic, R. Nikolic, D. Andjelkovic, and A. Bojic. 2006. A direct potentiometric titration study of the dissociation of humic acid with selectively blocked functional groups. Eclét. Quím. **31**: 39–46. doi:10.1590/S0100-46702006000300005

Badr, M. H., M. H. El-Halafawi, and E. R. Abd El-al Zeid. 2012. Comparison between the effect of ionic strength on acidity and dissociation constants of humic acids extracted from sewage sludge and nile water hyacinth composts. Glob. J. Environ. Res. **6**: 36–43.

Barbier, E. B., S. D. Hacker, C. Kennedy, E. W. Koch, A. C. Stier, and B. R. Silliman. 2011. The value of estuarine and coastal ecosystem services. Ecol. Monogr. **81**: 169–193.

Borges, A. V. 2005. Do we have enough pieces of the jigsaw to integrate CO_2 fluxes in the coastal ocean? Estuaries Coast **28**: 3–27.

Butman, D., and P. A. Raymond. 2011. Significant efflux of carbon dioxide from streams and rivers in the United States. Nat. Geosci. **4**: 839–842. doi:10.1038/NGEO1294

Cai, W.-J., Y. Wang, and R. E. Hodson. 1998. Acid-base properties of dissolved organic matter in the estuarine waters of Georgia, USA. Geochim. Cosmochim. Acta **62**: 473–483. doi:10.1016/S0016-7037(97)00363-3

Cai, W.-J., and others. 2011. Acidification of subsurface coastal waters enhanced by eutrophication. Nat. Geosci. **4**: 766–770. doi:10.1038/ngeo1297

Cole, J. J., N. Caraco, and G. Kling. 1994. Carbon dioxide supersaturation in the surface waters of lakes. Science **265**: 1568–1570.

Cronan, C. S., and G. R. Aiken. 1985. Chemistry and transport of soluble humic substances in forested watersheds of the Adirondack Park, New York. Geochim. Cosmochim. Acta **49**: 1697–1705. doi:10.1016/0016-7037(85)90140-1

Dickson, A. G. 1981. An exact definition of total alkalinity and a procedure for the estimation of alkalinity and total inorganic carbon from titration data. Deep-Sea Res. I Oceanogr. Res. Pap. **28**: 609–623. doi:10.1016/0198-0149(81)90121-7

Dickson, A. G. 1990. Thermodynamics of the dissociation of boric acid in synthetic seawater from 273.15 to 318.15 K. Deep-Sea Res. I Oceanogr. Res. Pap. **37**: 755–766. doi:10.1016/0198-0149(90)90004-F

Dickson, A. G., D. J. Wesolowski, D. A. Palmer, and R. E. Mesmer. 1990. Dissociation constant of bisulfate ion in aqueous sodium chloride solutions to 250 °C. J. Phys. Chem. **94**: 7978–7985. doi:10.1021/j100383a042

Dickson, A. G., J. D. Afghan, and G. C. Anderson. 2003. Reference materials for oceanic CO_2 analysis: A method for the certification of total alkalinity. Mar. Chem. **80**: 185–197. doi:10.1016/S0304-4203(02)00133-0

Dickson, A. G., C. L. Sabine, and J. R. Christian [eds.]. 2007. Guide to best practices for ocean CO_2 measurements, v. **3**. PICES Special Publication.

Douglas, N. K., and R. H. Byrne. 2017. Spectrophotometric pH measurements from river to sea: Calibration of mCP for $0 \le S \le 40$ and $278.15 \le T \le 308.15$K. Mar. Chem. **197**: 64–69. doi:10.1016/j.marchem.2017.10.001

Drever, J. I. 1997. The geochemistry of natural waters: Surface and groundwater environments. Prentice Hall.

Easley, R. A., and R. H. Byrne. 2012. Spectrophotometric calibration of pH electrodes in seawater using purified m-cresol purple. Environ. Sci. Technol. **46**: 5018–5024. doi:10.1021/es300491s

Eshleman, K. N., and H. F. Hemond. 1985. The role of organic acids in the acid-base status of surface waters at Bickford Watershed, Massachusetts. Water Resour. Res. **21**: 1503–1510. doi:10.1029/WR021i010p01503

Fahmy, S. H., S. W. R. Hann, and Y. Jiao. 2010. Soils of New Brunswick the second approximation. NBSWCC-PRC 2010-01. Eastern Canada Soil and Water Conservation Centre.

Gattuso, J.-P., J.-M. Epitalon, H. Lavigne and J. Orr. 2021. seacarb: seawater carbonate chemistry. R package version 3.3.0.The Comprehensive R Archive Network http://CRAN.R-project.org/package=seacarb

Gran, G. 1952. Determination of the equivalence point in potentiometric titrations. Part II. Analyst **77**: 661–671. doi:10.1039/AN9527700661

Hammer, K., B. Schneider, K. Kuliński, and D. E. Schulz-Bull. 2017. Acid-base properties of Baltic Sea dissolved organic matter. J. Mar. Syst. **173**: 114–121. doi:10.1016/j.jmarsys.2017.04.007

Hernández-Ayon, J. M., A. Zirino, A. G. Dickson, T. Camiro-Vargas, and E. Valenzuela-Espinoza. 2007. Estimating the contribution of organic bases from microalgae to the titration alkalinity in coastal seawaters. Limnol. Oceanogr.: Methods **5**: 225–232. doi:10.4319/lom.2007.5.225

Hinckley, J. A. 2021. The non-conservative behavior of organic alkalinity in U.S. and Canadian estuaries of the Gulf of Maine. Univ. of New Hampshire.

Hu, X., and W.-J. Cai. 2013. Estuarine acidification and minimum buffer zone—A conceptual study. Geophys. Res. Lett. **40**: 5176–5181. doi:10.1002/grl.51000

Hudson-Heck, E., and R. H. Byrne. 2022. Spectrophotometric analysis of the CO_2 system in aqueous solutions: A freshwater example from the Snake River, Idaho, USA. Limnol. Oceanogr.: Methods **20**: 741–753. doi:10.1002/lom3.10525

Hunt, C. W., J. E. Salisbury, and D. Vandemark. 2011. Contributions of non-carbonate anions to total alkalinity and overestimation of pCO_2 in New England and New Brunswick rivers. Biogeosciences **8**: 3069–3076. doi:10.5194/bg-8-3069-2011

Hunt, C. W., J. E. Salisbury, and D. Vandemark. 2013. CO_2 input dynamics and air–sea exchange in a large New England estuary. Estuaries Coast **37**: 1078–1091. doi:10.1007/s12237-013-9749-2

Keller, J. 2020. Taking stock of a Downeast river. Island Institute, [accessed 2020 March 5]. Available from http://www.islandinstitute.org/working-waterfront/taking-stock-downeast-river

Kerr, D. E., C. Turner, A. Grey, J. Keogh, P. J. Brown, and B. P. Kelleher. 2023*a*. OrgAlkCalc: Estimation of organic alkalinity quantities and acid-base properties with proof of concept in Dublin Bay. Mar. Chem. **251**: 104234. doi:10.1016/j.marchem.2023.104234

Kerr, D. E., A. Grey, and B. P. Kelleher. 2023*b*. Organic alkalinity dynamics in Irish coastal waters: Case study Rogerstown Estuary. Mar. Chem. **254**: 104272. doi:10.1016/j.marchem.2023.104272

Ko, Y. H., K. Lee, K. H. Eom, and I.-S. Han. 2016. Organic alkalinity produced by phytoplankton and its effect on the computation of ocean carbon parameters. Limnol. Oceanogr. **61**: 1462–1471. doi:10.1002/lno.10309

Kuliński, K., B. Schneider, K. Hammer, U. Machulik, and D. Schulz-Bull. 2014. The influence of dissolved organic matter on the acid–base system of the Baltic Sea. J. Mar. Syst. **132**: 106–115. doi:10.1016/j.jmarsys.2014.01.011

Lewis, E., and D. W. R. Wallace. 1998. Program developed for CO_2 system calculations. Carbon Dioxide Information Analysis Center, Report ORNL/CDIAC-105. Oak Ridge National Laboratory.

Liu, X., M. C. Patsavas, and R. H. Byrne. 2011. Purification and characterization of meta-cresol purple for spectrophotometric seawater pH measurements. Environ. Sci. Technol. **45**: 4862–4868. doi:10.1021/es200665d

Lozovik, P. A. 2005. Contribution of organic acid anions to the alkalinity of natural humic water. J. Anal. Chem. **60**: 1000–1004. doi:10.1007/s10809-005-0226-3

Martell-Bonet, L., and R. H. Byrne. 2023. A differential titration method for determining the dissociation characteristics of natural organic acids in the coastal zone. Chem. Geol. **636**: 121634. doi:10.1016/j.chemgeo.2023.121634

McDonald, C. P., E. G. Stets, R. G. Striegl, and D. Butman. 2013. Inorganic carbon loading as a primary driver of dissolved carbon dioxide concentrations in the lakes and reservoirs of the contiguous United States. Global Biogeochem. Cycles **27**: 285–295.

Millero, F. J. 2010. Carbonate constants for estuarine waters. Mar. Freshwater Res. **61**: 139–142. doi:10.1071/MF09254

Nixon, S. W. 1995. Coastal marine eutrophication: A definition, social causes, and future concerns. Ophelia **41**: 199–219. doi:10.1080/00785236.1995.10422044

Park, P. K. 1960. Oceanic CO_2 system: An evaluation of ten methods of investigation. Limnol. Oceanogr. **14**: 179–186.

Paxéus, N., and M. Wedborg. 1985. Acid-base properties of aquatic fulvic acid. Anal. Chim. Acta **169**: 87–98. doi:10.1016/S0003-2670(00)86210-8

Raymond, P. A., and others. 2013. Global carbon dioxide emissions from inland waters. Nature **503**: 355–359.

Sharp, J. D., and R. H. Byrne. 2020. Interpreting measurements of total alkalinity in marine and estuarine waters in the presence of proton-binding organic matter. Deep-Sea Res. I Oceanogr. Res. Pap. **165**: 103338. doi:10.1016/j.dsr.2020.103338

Sharp, J. D., and R. H. Byrne. 2021. Technical note: Excess alkalinity in carbonate system reference materials. Mar. Chem. 233: 103965. doi:10.1016/j.marchem.2021.103965

Sippo, J. Z., D. T. Maher, D. R. Tait, C. Holloway, and I. R. Santos. 2016. Are mangroves drivers or buffers of coastal acidification? Insights from alkalinity and dissolved inorganic carbon export estimates across a latitudinal transect. Global Biogeochem. Cycles **30**: 753–766. doi:10.1002/2015GB005324

Song, S., Z. A. Wang, M. E. Gonneea, K. D. Kroeger, S. N. Chu, D. Li, and H. Liang. 2020. An important biogeochemical link between organic and inorganic carbon cycling: Effects of organic alkalinity on carbonate chemistry in coastal waters influenced by intertidal salt marshes. Geochim. Cosmochim. Acta **275**: 123–139. doi:10.1016/j.gca.2020.02.013

Song, S., R. G. James Bellerby, Z. A. Wang, E. Wurgaft, and D. Li. 2023. Organic alkalinity as an important constituent of total alkalinity and the buffering system in river-to-coast transition zones. J. Geophys. Res. Oceans **128**: e2022JC019270. doi:10.1029/2022JC019270

Strickland, J. D. H. and T. R. Parsons. 1972. A Practical Handbook of Seawater Analysis. 2nd edn. Fisheries Research Board of Canada, 310pp. (Bulletin Fisheries Research Board of Canada, Nr. 167 (2nd ed)). DOI:http://dx.doi.org/10.25607/OBP-1791

Stumm, W., and J. J. Morgan. 1995. Aquatic chemistry: Chemical equilibria and rates in natural waters, 3rd ed. Wiley-Interscience.

Ulfsbo, A., K. Kuliński, L. G. Anderson, and D. R. Turner. 2015. Modelling organic alkalinity in the Baltic Sea using a Humic-Pitzer approach. Mar. Chem. **168**: 18–26. doi:10.1016/j.marchem.2014.10.013

Uppström, L. R. 1974. The boron/chlorinity ratio of deep-sea water from the Pacific Ocean. Deep-Sea Res. Oceanogr. Abstr. **21**: 161–162. doi:10.1016/0011-7471(74)90074-6

Van Heuven, S., D. Pierrot, J. W. B. Rae, E. Lewis, and D. W. R. Wallace. 2017. CO2SYS v 1.1, MATLAB program developed for CO_2 system calculations. ORNL/CDIAC-105b. Oak Ridge National Laboratory, U.S. Department of Energy.

Waldbusser, G. G., and J. E. Salisbury. 2014. Ocean acidification in the coastal zone from an organism's perspective: Multiple system parameters, frequency domains, and habitats. Ann. Rev. Mar. Sci. **6**: 221–247.

Wang, Z. A., K. D. Kroeger, N. K. Ganju, M. E. Gonneea, and S. N. Chu. 2016. Intertidal salt marshes as an important source of inorganic carbon to the coastal ocean. Limnol. Oceanogr. **61**: 1916–1931. doi:10.1002/lno.10347

Yang, B., R. H. Byrne, and M. Lindemuth. 2015. Contributions of organic alkalinity to total alkalinity in coastal waters: A spectrophotometric approach. Mar. Chem. **176**: 199–207. doi:10.1016/j.marchem.2015.09.008

Acknowledgments

We thank Brian Beal and Jeff Robinson of the Downeast Institute for their support in Pleasant estuary sampling, and the crew of DMK Marine for St. John sampling support. We gratefully thank Shawn Shellito for tireless help in fieldwork and Megan Molinari for dedication to laboratory analysis, and two reviewers for their thoughtful suggestions. This work was funded by NSF Awards 1658377 and 1658321.

Conflict of interest

The authors declare no conflicts of interest.

Submitted 08 April 2024
Revised 07 August 2024
Accepted 20 November 2024

Associate editor: Robinson Fulweiler